

2D mapping of the physical and chemical properties of the ionized gas in NGC 5253



Ana Monreal-Ibero⁽¹⁾

J. Walsh⁽²⁾, J.M. Vílchez⁽¹⁾

⁽¹⁾IAA, ⁽²⁾ESO

(based mainly – but not only – on Monreal-Ibero et al. 2012, A&A, 544, 60)



2D mapping of the physical and chemical properties of the ionized gas in NGC 5253



Ana Monreal-Ibero⁽¹⁾

J. Walsh⁽²⁾, J.M. Vílchez⁽¹⁾

⁽¹⁾IAA, ⁽²⁾ESO

(based mainly – but not only – on Monreal-Ibero et al. 2012, A&A, 544, 60)



Intro: Blue Compact Dwarfs

Dwarf Irregular Galaxy NGC 1705



Hubble
Heritage

- Dwarf: $M_B > -18$
- Compact: $\emptyset < 1 \text{ kpc}$
- With bright emission lines similar to those in HII regions
- With massive SF
- Low metallicity

BCDs are ideal laboratories to study the interplay between massive SF and surrounding gas

Intro: Blue Compact Dwarfs

Dwarf Irregular Galaxy NGC 1705



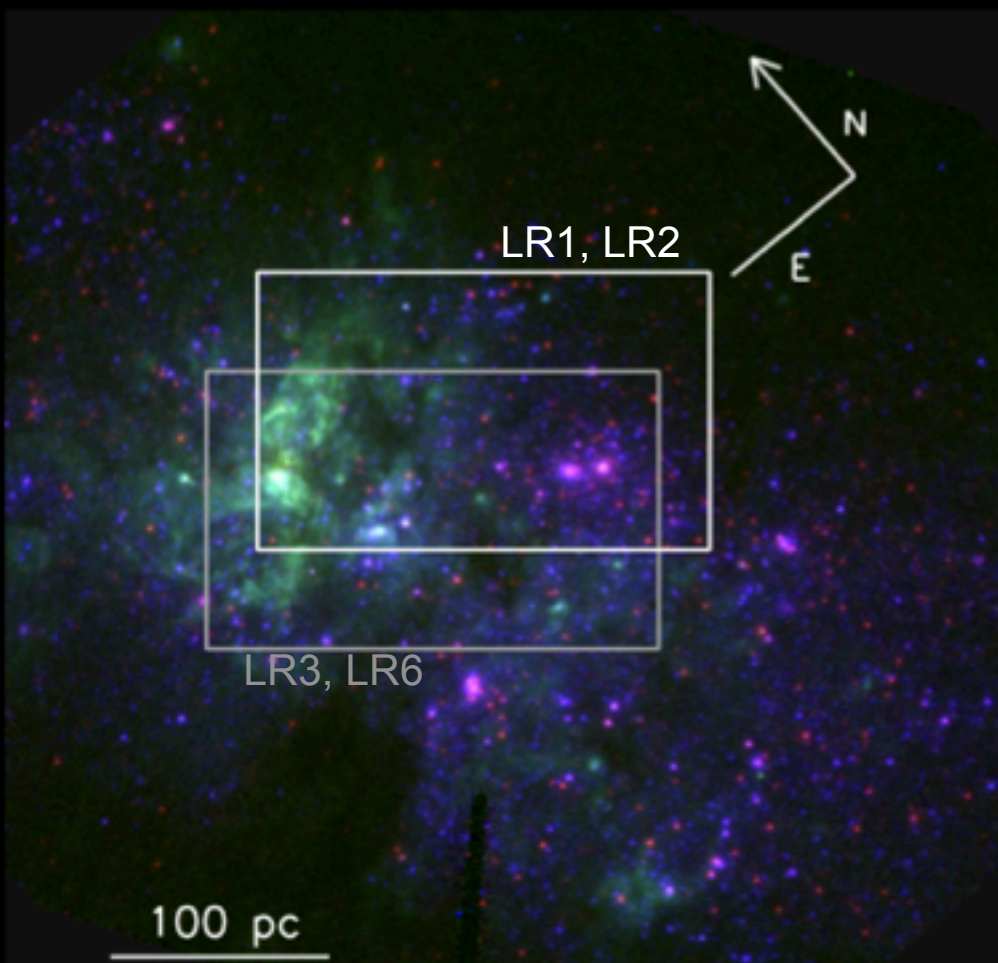
Hubble
Heritage

NASA, ESA, and The Hubble Heritage Team (STScI/AURA) • Hubble Space Telescope WFC2 • STScI-PRC03-07

- Dwarf: $M_B > -18$
- Compact: $\varnothing < 1 \text{ kpc}$
- With bright emission lines similar to those in HII regions
- With massive SF
- Low metallicity

BCDs are ideal laboratories to study the interplay between massive SF and surrounding gas

NGC 5253

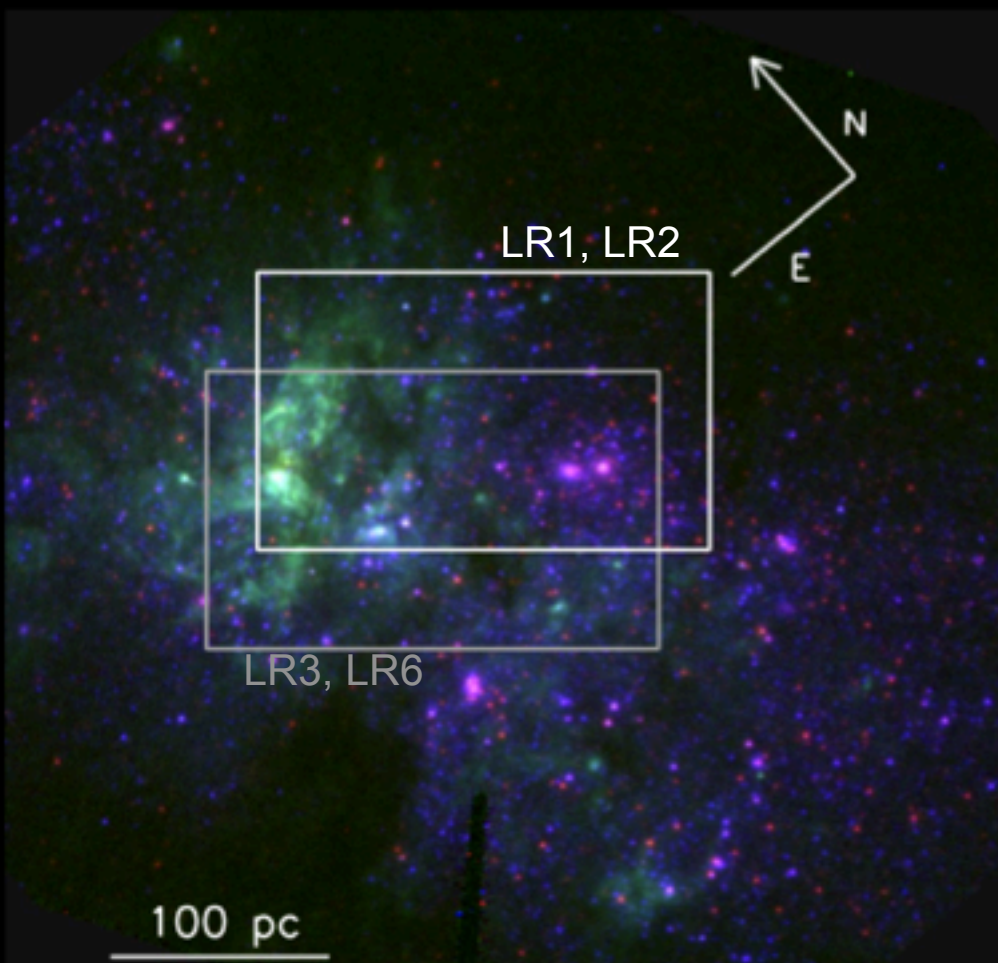


- Very close; D=3.8 Mpc; z=0.001358
- Scale=18.4pc/"
- $M_B=-17.13$
- $M(HI)=1.4 \times 10^8 M_\odot$
- Filamentary structure
- Hints of inflows/ouflows
- Reported extra N, WR emission etc.
- Complex kinematics
- $Z \sim 0.3 Z_\odot$

(HST-ACS, I+H α +B, program 10609, P.I.: Vacca)

We want to see the details. Let's look at it with IFS.

NGC 5253



- Very close; D=3.8 Mpc; z=0.001358
- Scale=18.4pc/"
- $M_B=-17.13$
- $M(HI)=1.4 \times 10^8 M_\odot$
- Filamentary structure
- Hints of inflows/ouflows
- Reported extra N, WR emission etc.
- Complex kinematics

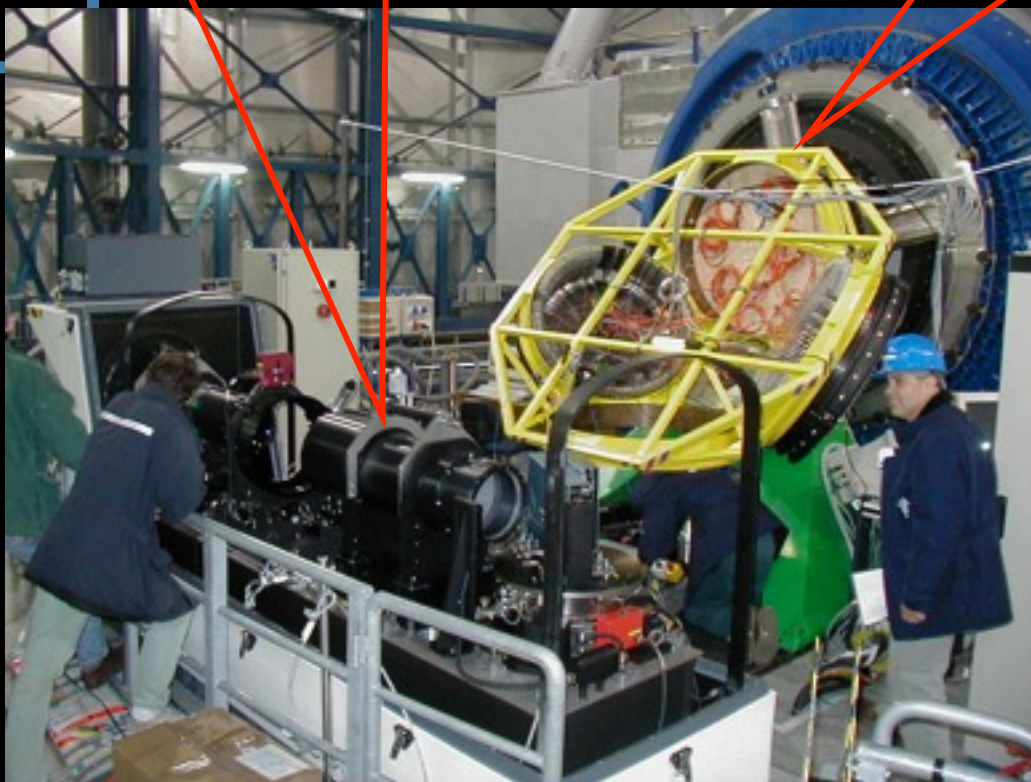
(HST-ACS, I+H α +B, program 10609, P.I.: Vacca)

We want to see the details. Let's look at it with IFS.

FLAMES@VLT

GIRAFFE: The spectrograph

OzPoz: The fiber positioner



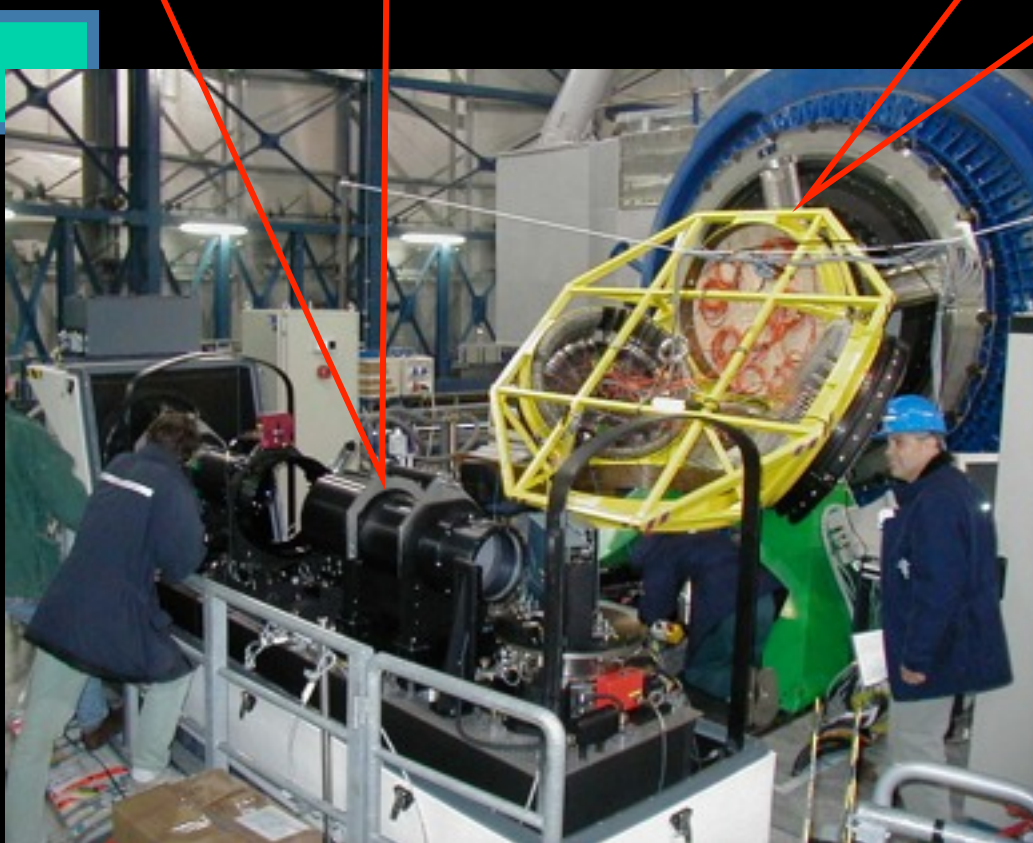
ARGUS mode:
•scaling: 0.52"/spa;
•f.o.v.: 11.5"x7.3"

Grating	R	$\Delta\lambda$ (nm)	t_{exp} (s)
LR1	12800	361-408	21x895
LR2	10200	369-456	9x895
LR3	12000	450-508	5x1500
LR6	13700	644-718	5x1500

FLAMES@VLT

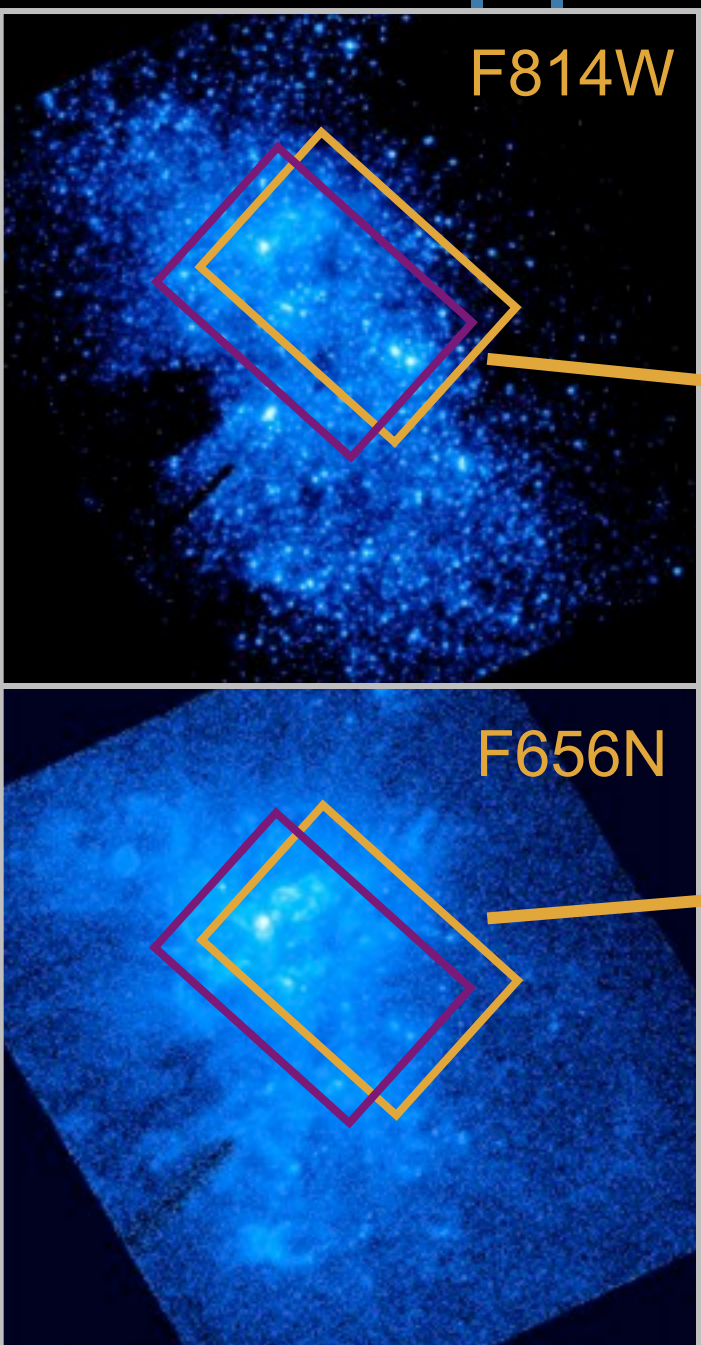
GIRAFFE: The spectrograph

OzPoz: The fiber positioner

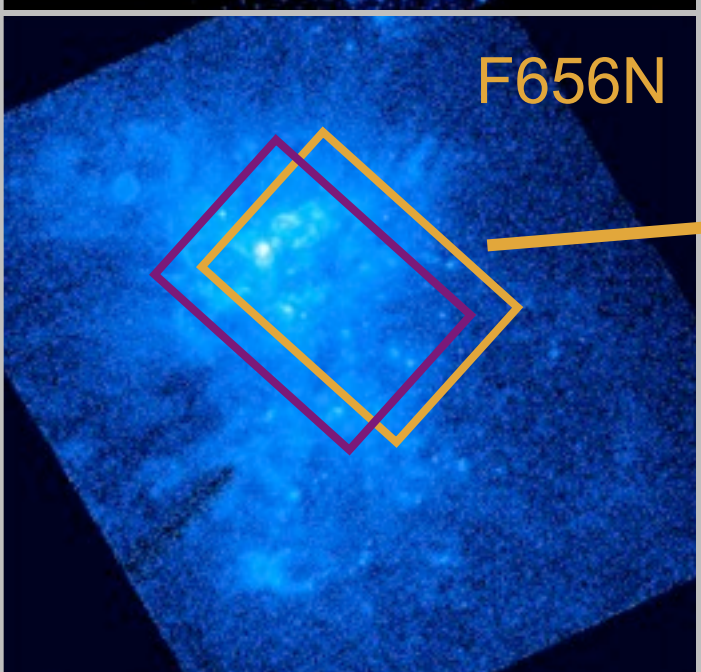


ARGUS mode:
•scaling: 0.52"/spa;
•f.o.v.: 11.5" x 7.3"

Grating	R	$\Delta\lambda$ (nm)	t_{exp} (s)
LR1	12800	361-408	21x895
LR2	10200	369-456	9x895
LR3	12000	450-508	5x1500
LR6	13700	644-718	5x1500

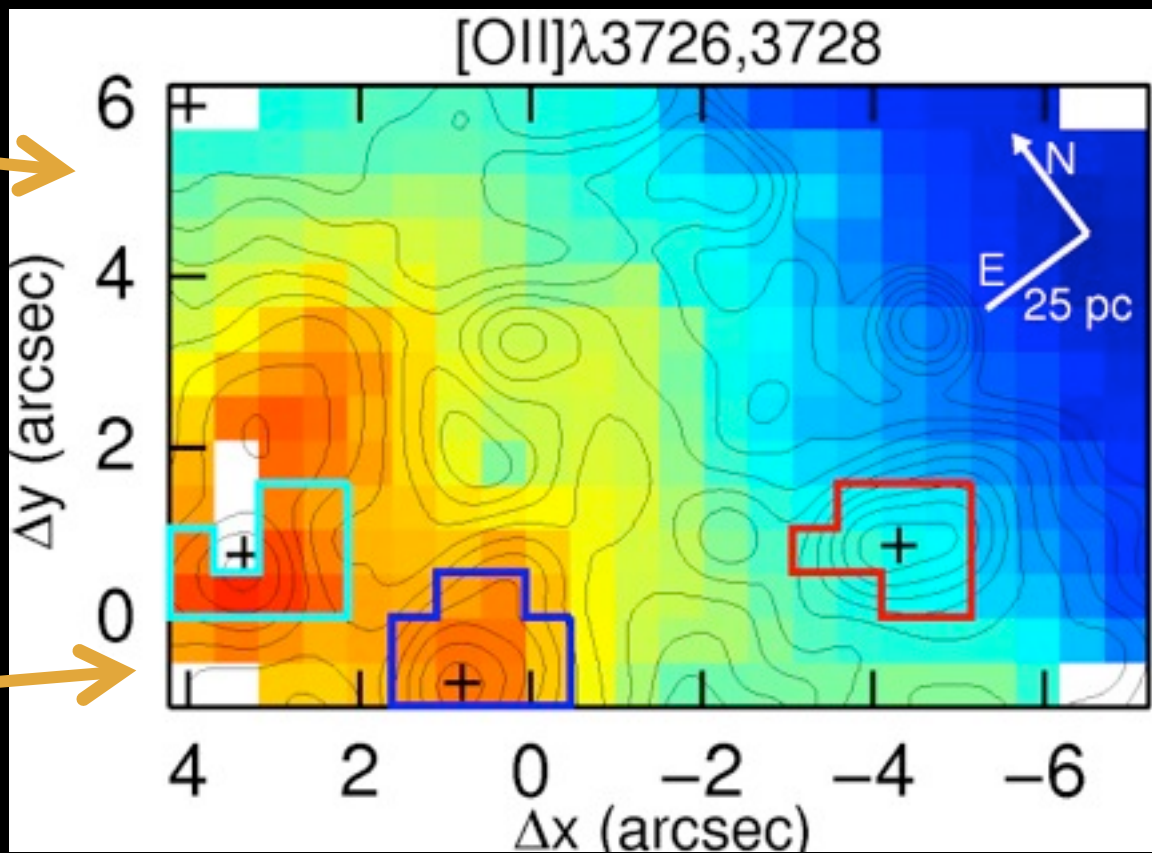


F814W

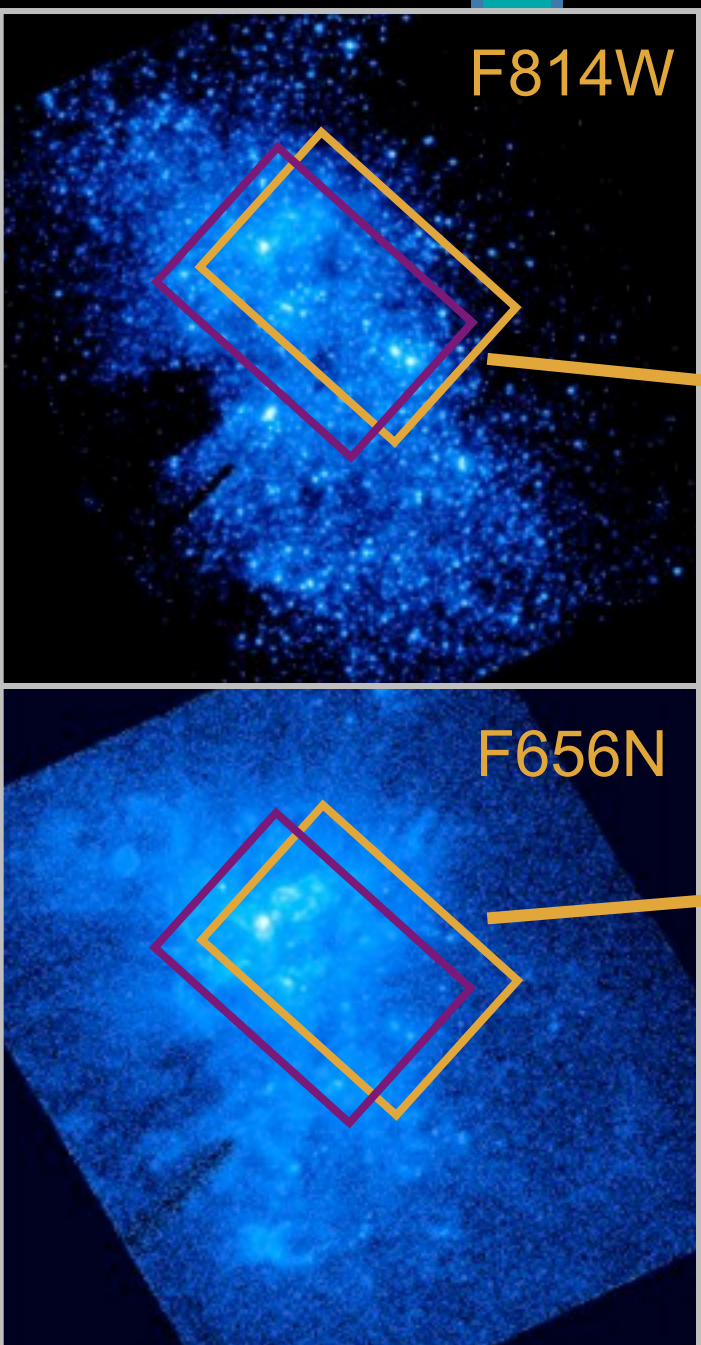


F656N

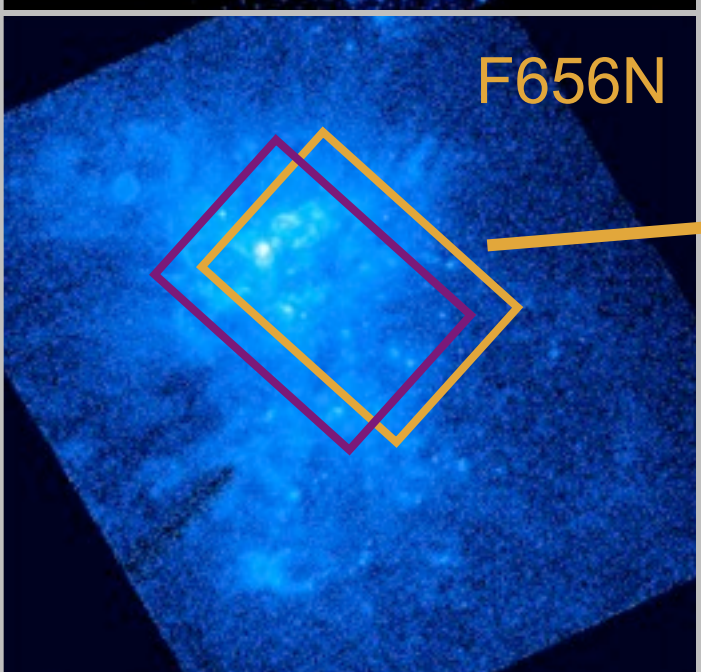
Where are we?



□ 1 spa $\sim 10 \text{ pc} \times 10 \text{ pc}$

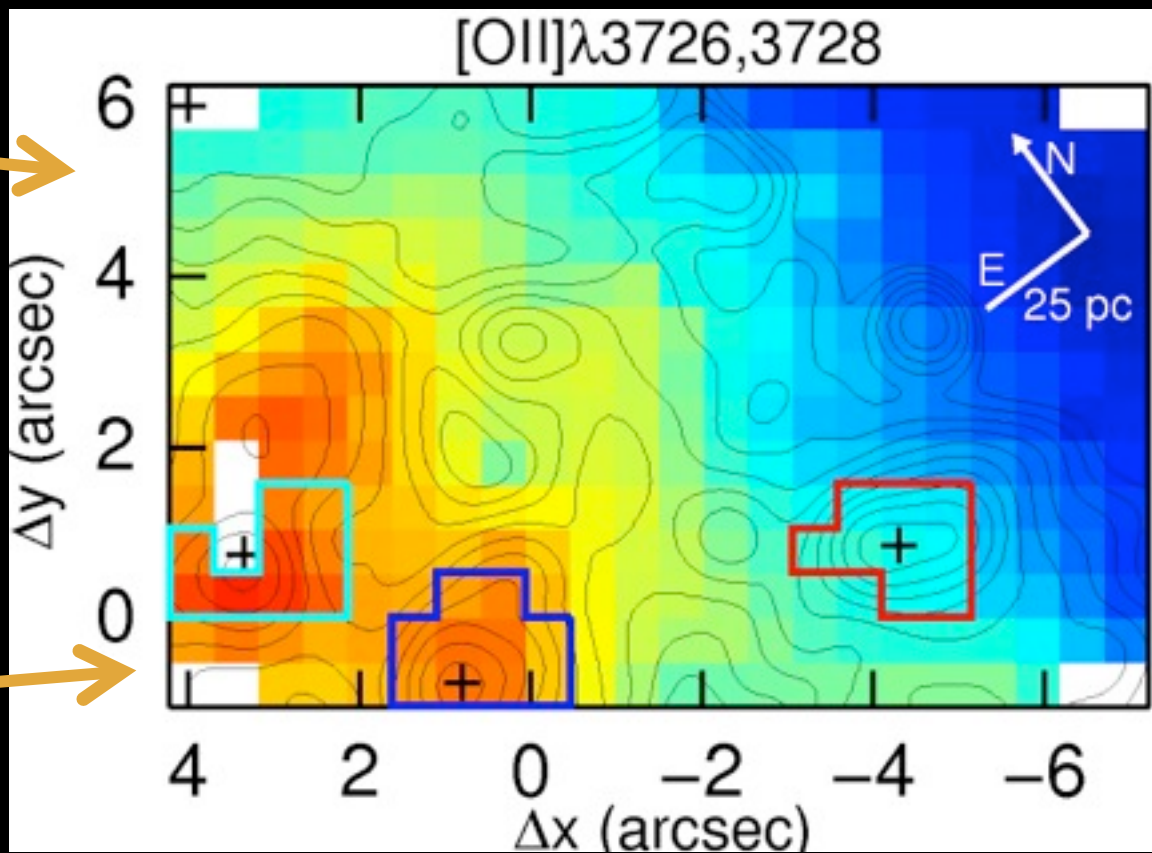


F814W



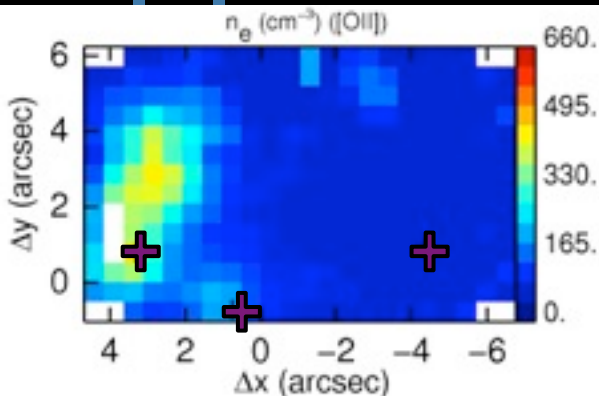
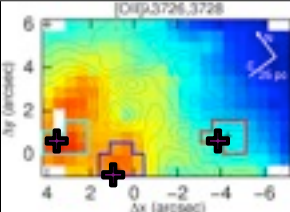
F656N

Where are we?

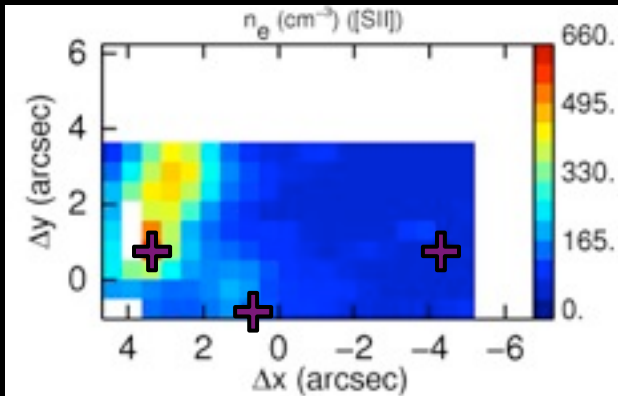


□ 1 spa $\sim 10 \text{ pc} \times 10 \text{ pc}$

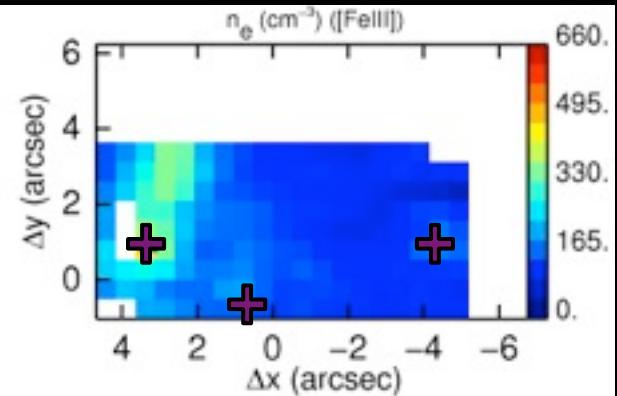
Electron density



$\lambda 3726/\lambda 3729$



$\lambda 6717/\lambda 6731$

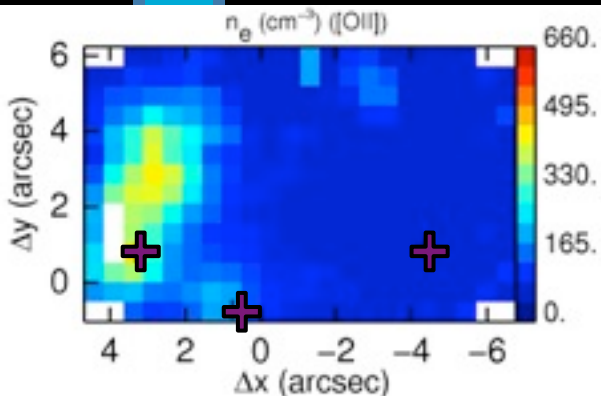
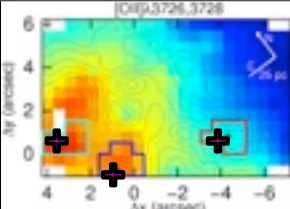


$\lambda 4986/\lambda 4658$

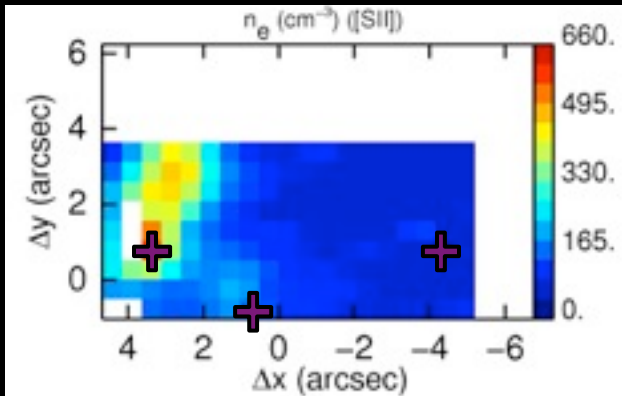
- Most of the f.o.v.: < low density limit
- Knot 2: $\sim 190 \text{ cm}^{-3}$
- GHIIR: The richest structure
 - the largest n_e .
 - 2 peaks
 - $n_e([\text{SII}]) > n_e([\text{OII}]) \sim n_e([\text{FeIII}])$



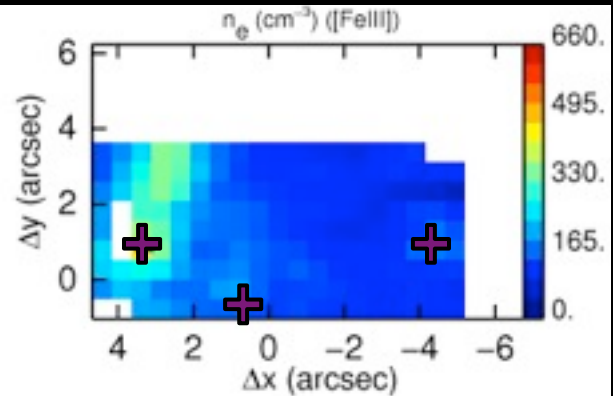
Electron density



$\lambda 3726/\lambda 3729$



$\lambda 6717/\lambda 6731$

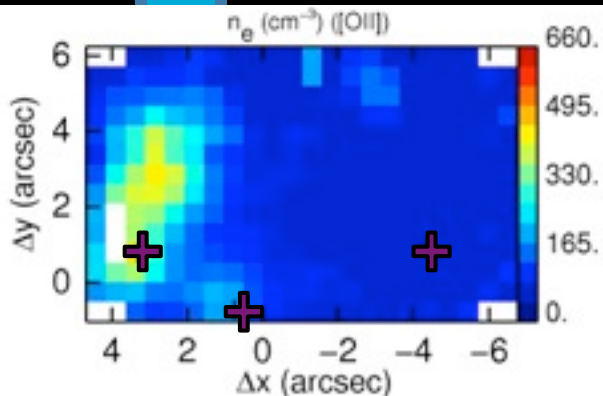
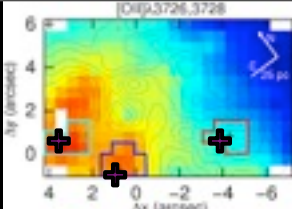


$\lambda 4986/\lambda 4658$

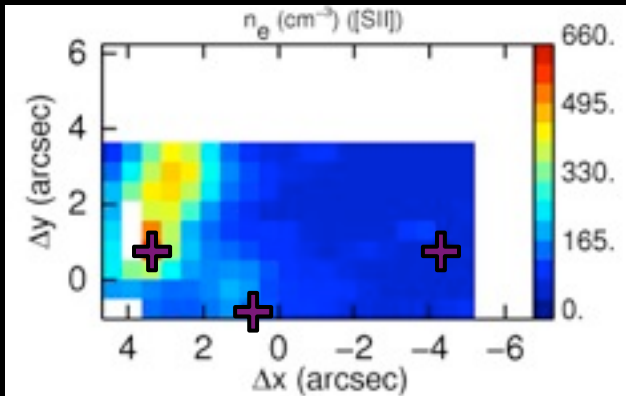
- Most of the f.o.v.: < low density limit
- Knot 2: $\sim 190 \text{ cm}^{-3}$
- GHIIR: The richest structure
 - the largest n_e .
 - 2 peaks
 - $n_e([\text{SII}]) > n_e([\text{OIII}]) \sim n_e([\text{FeIII}])$



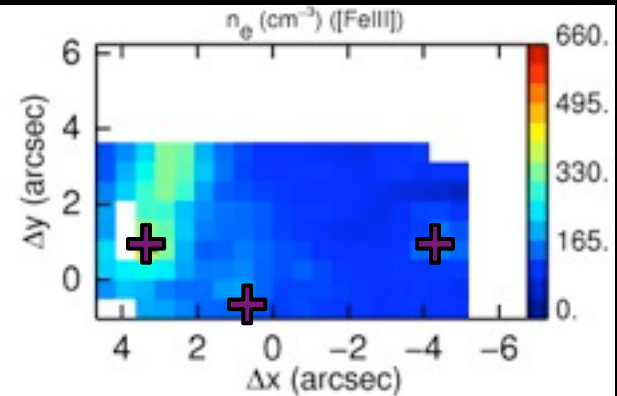
Electron density



$\lambda 3726/\lambda 3729$



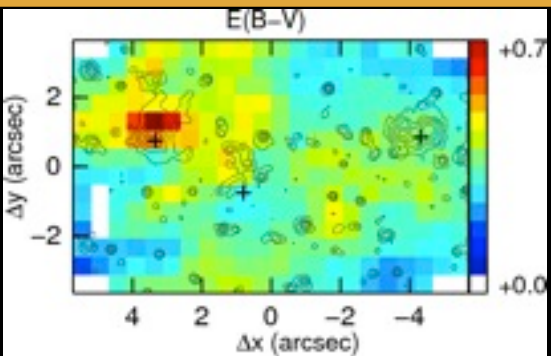
$\lambda 6717/\lambda 6731$



$\lambda 4986/\lambda 4658$

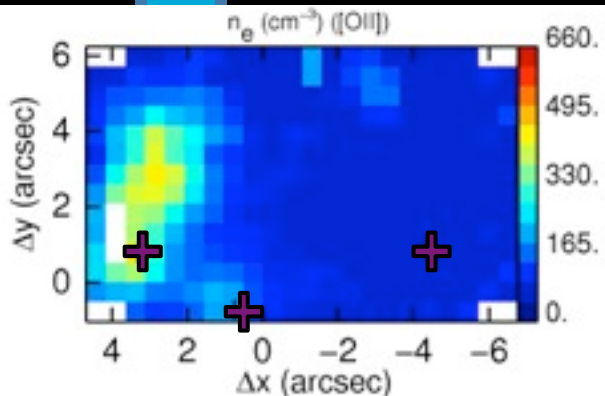
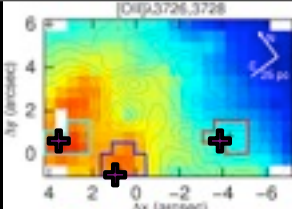
- Most of the f.o.v.: < low density limit
- Knot 2: $\sim 190 \text{ cm}^{-3}$
- GHIIR: The richest structure
 - the largest n_e .
 - 2 peaks
 - $n_e([\text{SII}]) > n_e([\text{OII}]) \sim n_e([\text{FeIII}])$

+ heavy extinction in the GHIIR

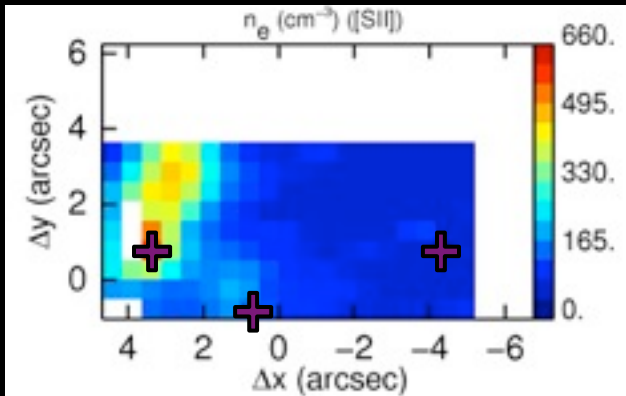


(Monreal-Ibero et al.
2010, A&A, 517, 27)

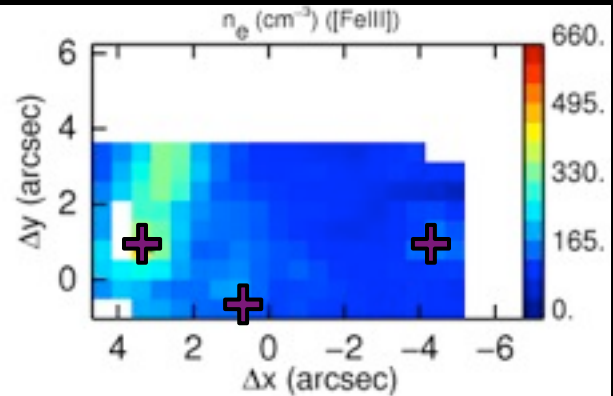
Electron density



$\lambda 3726/\lambda 3729$



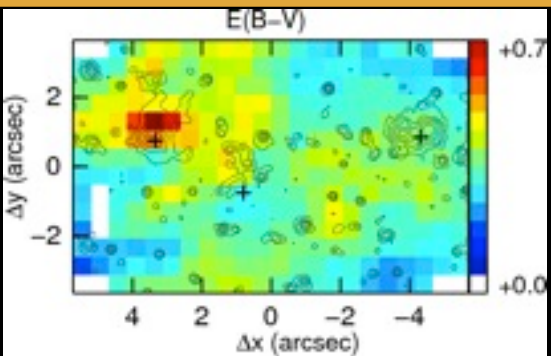
$\lambda 6717/\lambda 6731$



$\lambda 4986/\lambda 4658$

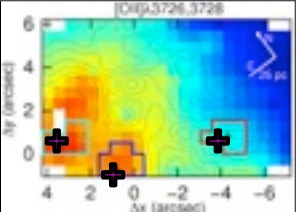
- Most of the f.o.v.: < low density limit
- Knot 2: $\sim 190 \text{ cm}^{-3}$
- GHIIR: The richest structure
 - the largest n_e .
 - 2 peaks
 - $n_e([\text{SII}]) > n_e([\text{OIII}]) \sim n_e([\text{FeIII}])$

+ heavy extinction in the GHIIR

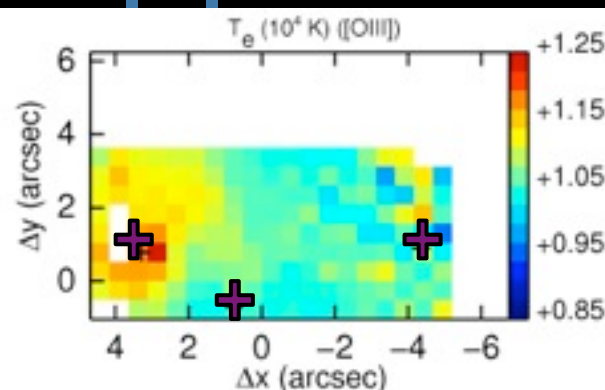


(Monreal-Ibero et al.
2010, A&A, 517, 27)

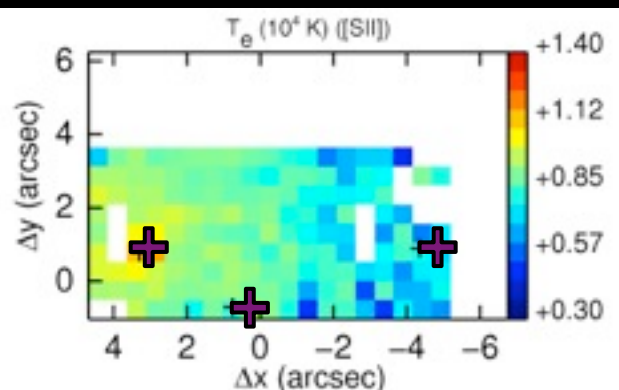
Results consistent with an onion-like structure where the inner layers are denser than the outer ones.



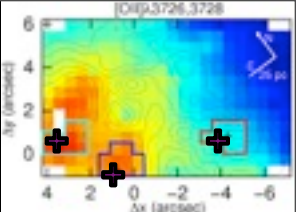
Electron temperature



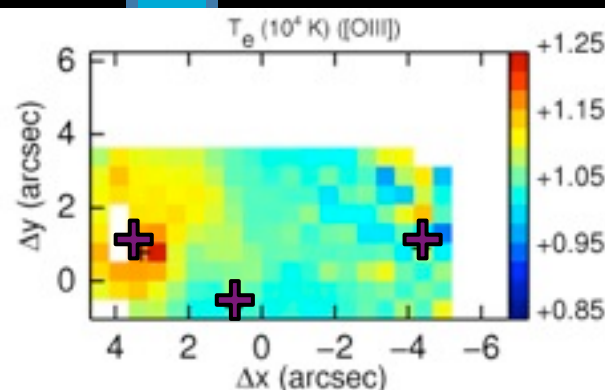
$\lambda\lambda 4959, 5007 / \lambda 4343$



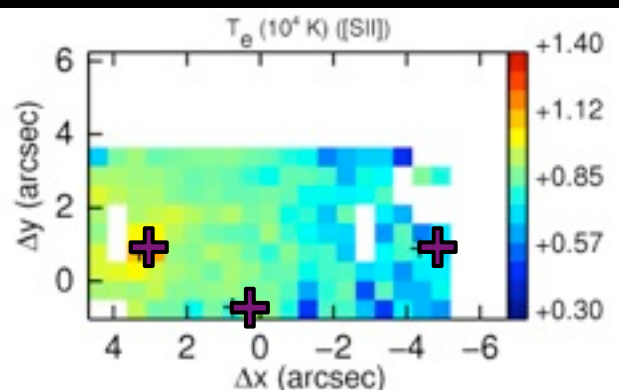
$\lambda\lambda 6717, 6731 / \lambda\lambda 4069, 4076$



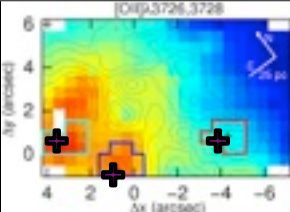
Electron temperature



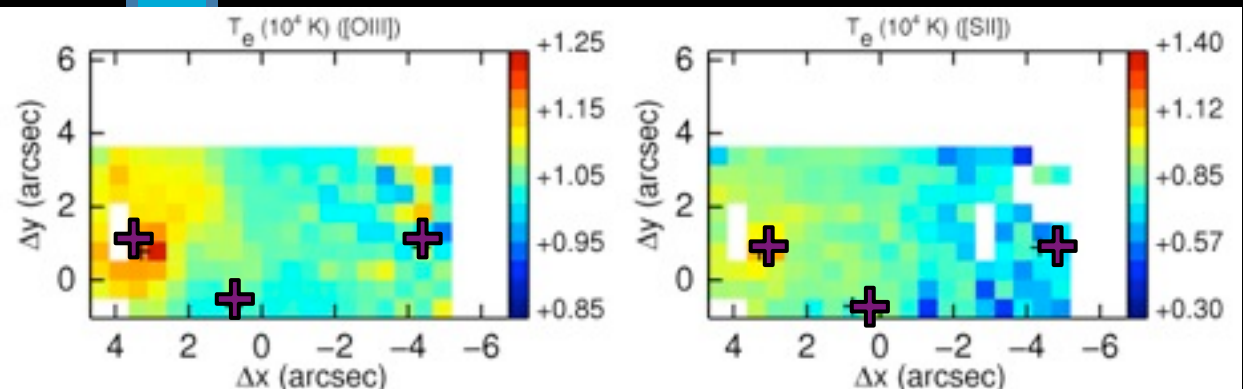
$\lambda\lambda 4959, 5007 / \lambda 4343$



$\lambda\lambda 6717, 6731 / \lambda\lambda 4069, 4076$



Electron temperature

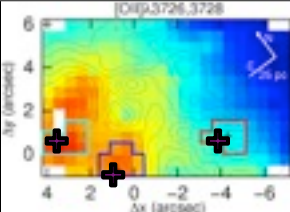


$\lambda\lambda 4959, 5007 / \lambda 4343$

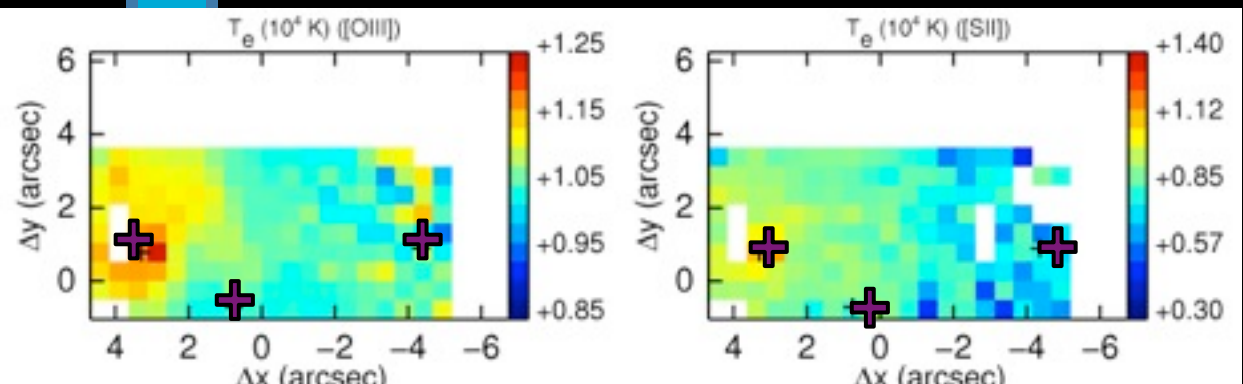
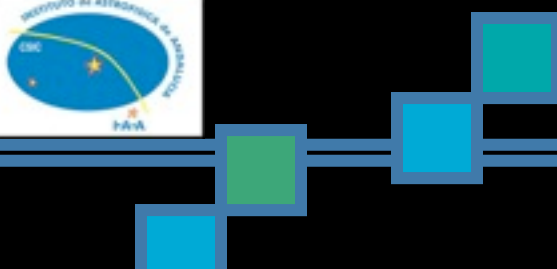
$\lambda\lambda 6717, 6731 / \lambda\lambda 4069, 4076$

- Similar structure in both maps
 - Largest T_e at peak in H α
 - Decreasing outwards
- $T_e([\text{SII}]) \sim 0.6\text{-}0.8 T_e([\text{OIII}])$
 - $T_e([\text{OIII}]) = 10000 - 12000 \text{ K}$
 - $T_e([\text{SII}]) = 6000 - 11000 \text{ K}$



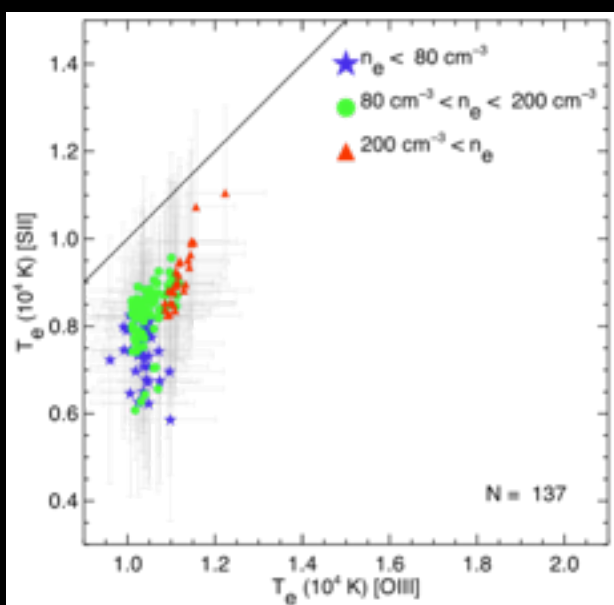


Electron temperature



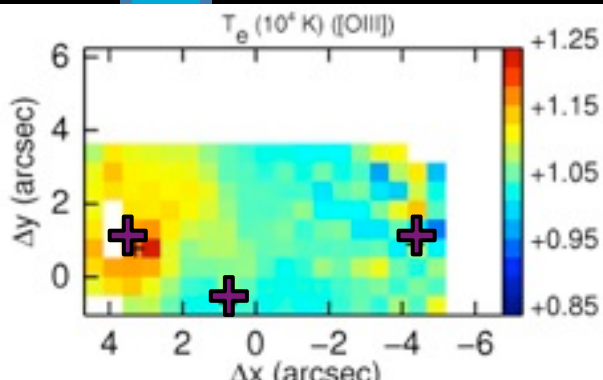
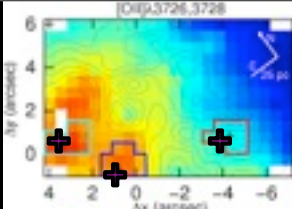
$\lambda\lambda 4959, 5007/\lambda 4343$

$\lambda\lambda 6717, 6731/\lambda\lambda 4069, 4076$

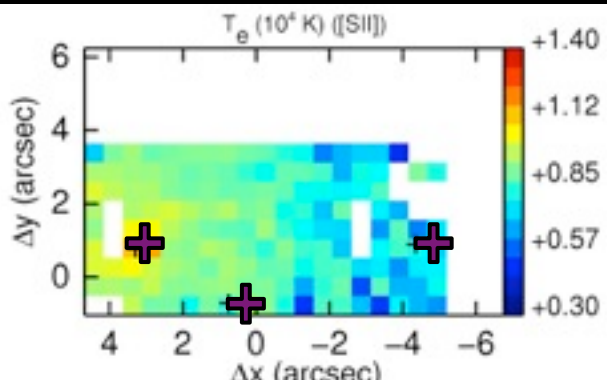


- Similar structure in both maps
 - Largest T_e at peak in H α
 - Decreasing outwards
- $T_e([\text{SII}]) \sim 0.6\text{-}0.8 T_e([\text{OIII}])$
 - $T_e([\text{OIII}]) = 10000 - 12000 \text{ K}$
 - $T_e([\text{SII}]) = 6000 - 11000 \text{ K}$

Electron temperature

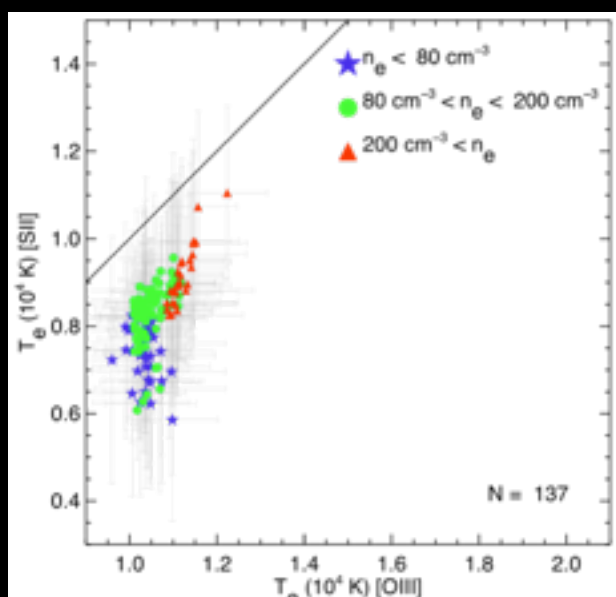


$\lambda\lambda 4959, 5007 / \lambda 4343$



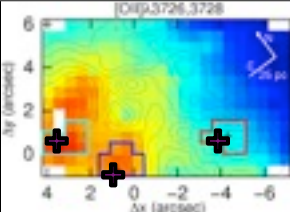
$\lambda\lambda 6717, 6731 / \lambda\lambda 4069, 4076$

(1) (2)

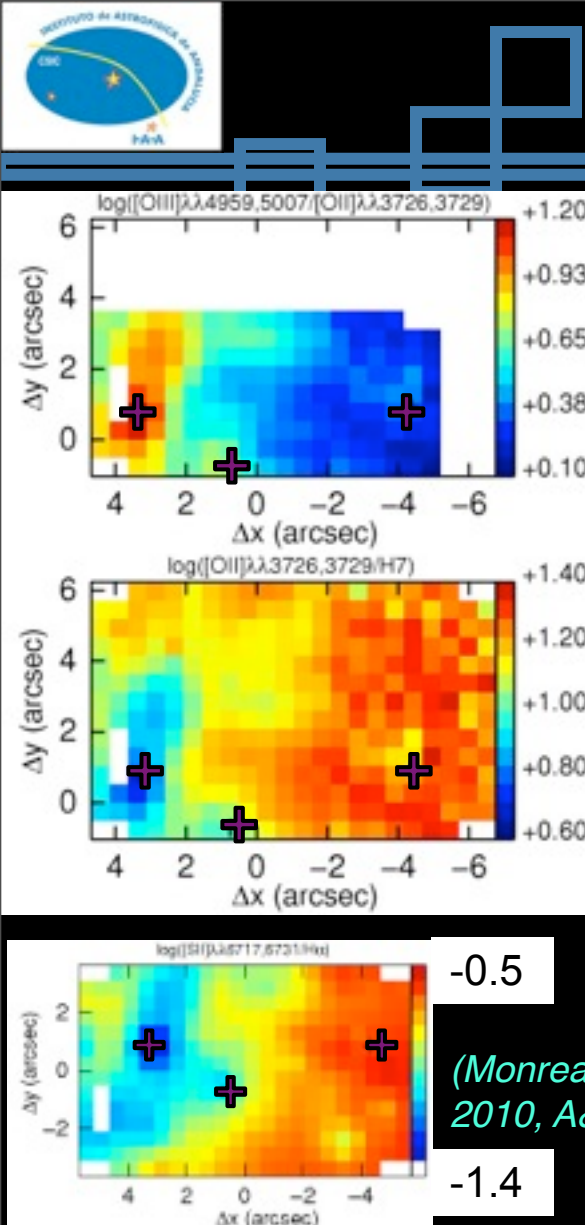


- Similar structure in both maps
 - Largest T_e at peak in H α
 - Decreasing outwards
- $T_e([\text{SII}]) \sim 0.6\text{-}0.8 T_e([\text{OIII}])$
 - $T_e([\text{OIII}]) = 10000 - 12000 \text{ K}$
 - $T_e([\text{SII}]) = 6000 - 11000 \text{ K}$

Both, (1) and (2) are consistent with a T_e structure in 3D with higher temperatures close to the main ionizing source surrounded by a more diffuse component of ionized gas at lower T_e .



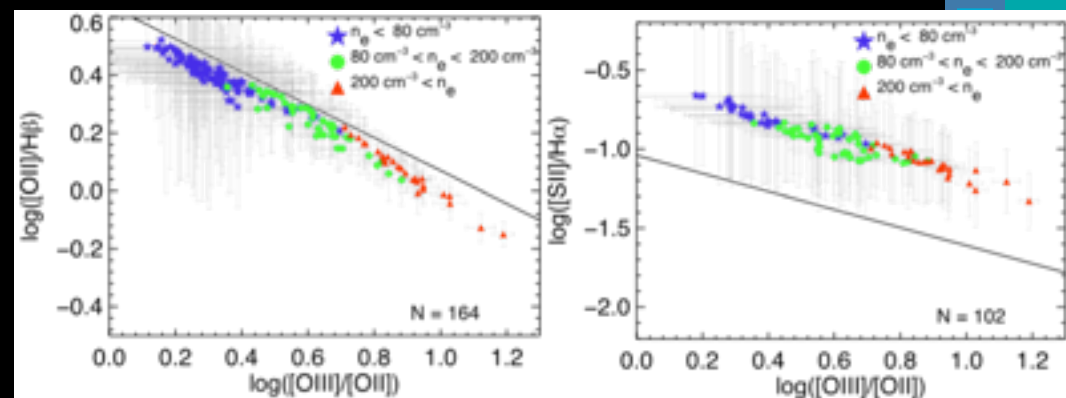
Local ionization degree



- The ionization structure reproduces the morphology observed for the ionized gas
- Similar structure in all the 3 utilized maps suggest a lack of any metallicity gradient.
- When comparing with models from literature, [SII]/H α disagrees

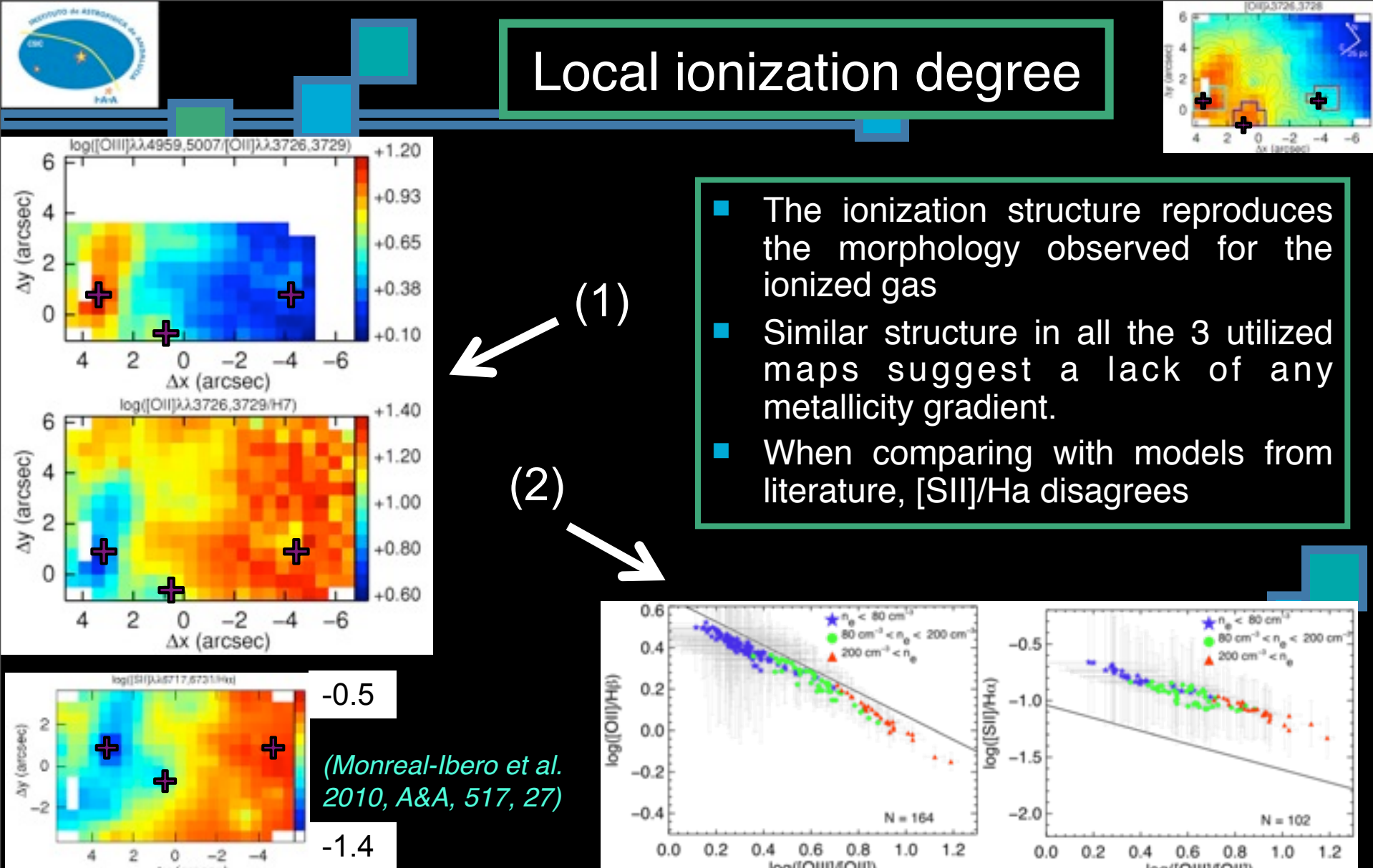
(1)

(2)



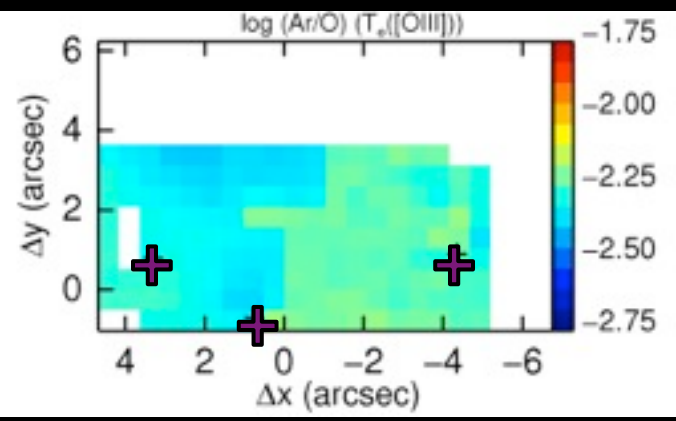
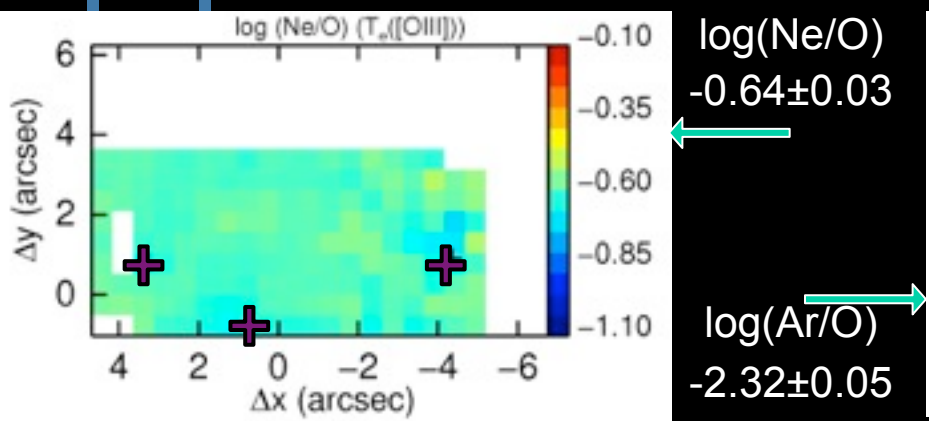
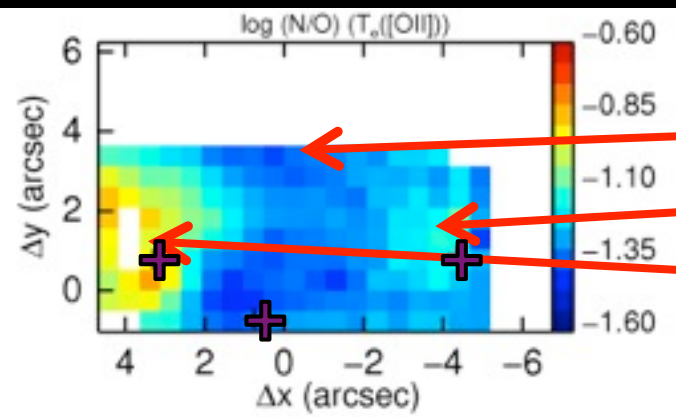
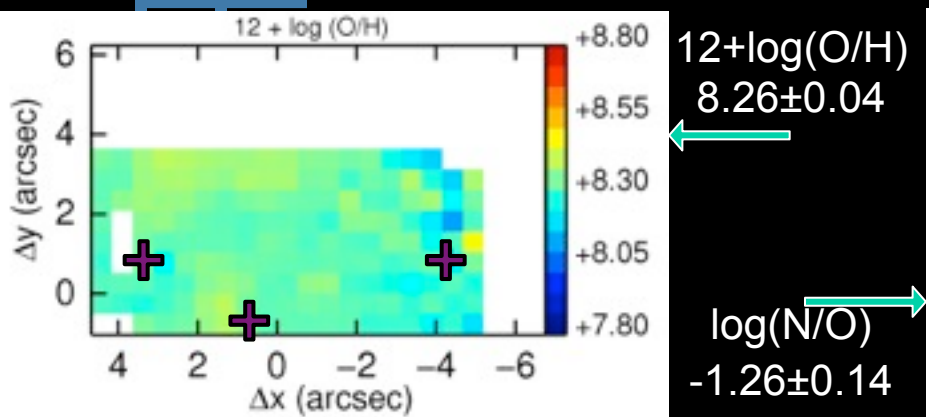
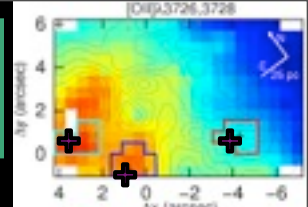
A possible 3D interpretation of (1) and (2) is that we are seeing how the lower ionizations species delineate the more extended diffuse component.

Local ionization degree



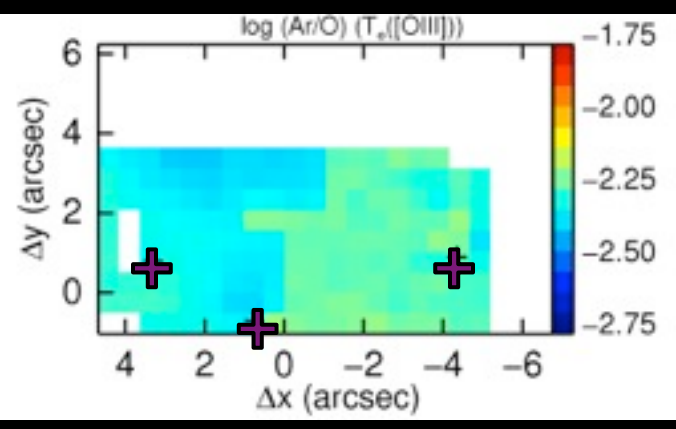
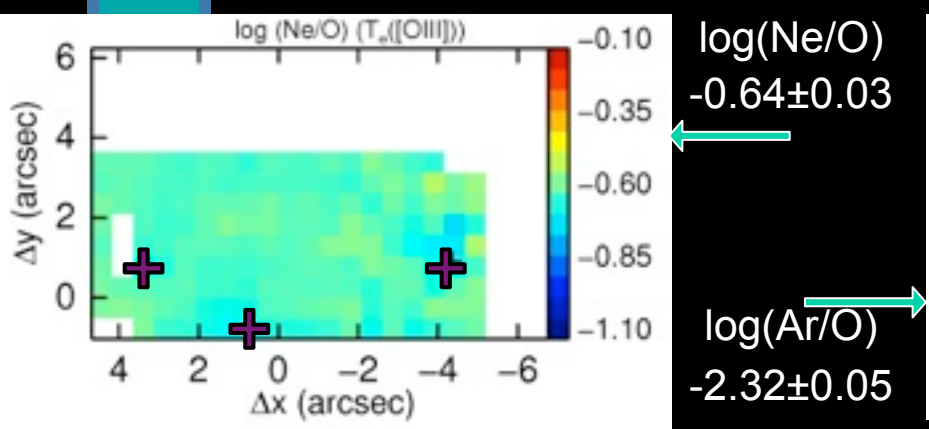
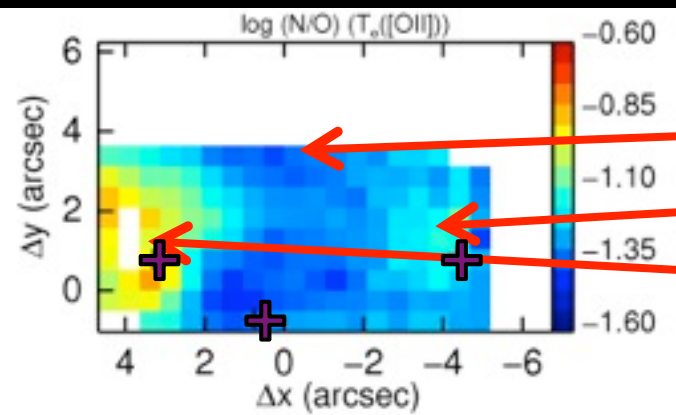
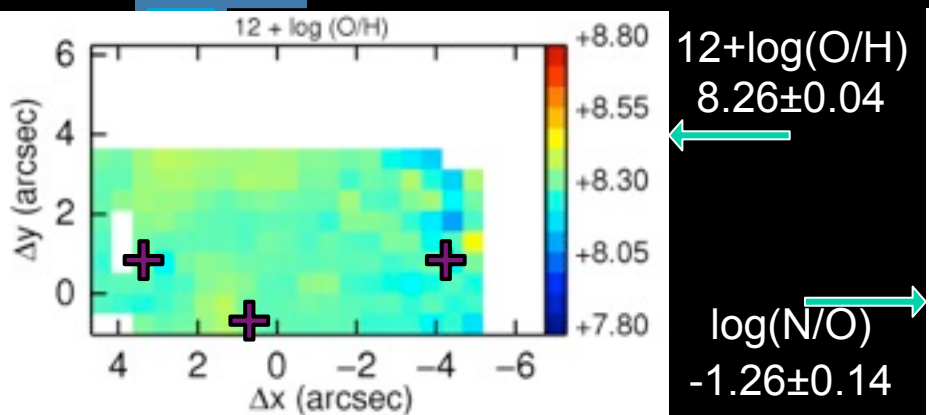
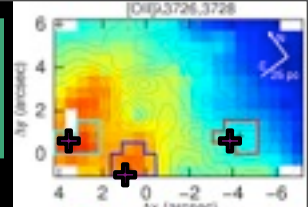
A possible 3D interpretation of (1) and (2) is that we are seeing how the lower ionizations species delineate the more extended diffuse component.

Abundances of heavy elements

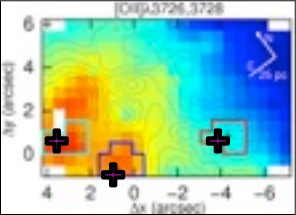


- Oxygen, neon, and argon present homogeneous abundances within 0.1 dex
- Nitrogen abundance has a complex structure with two areas of N-enhancement

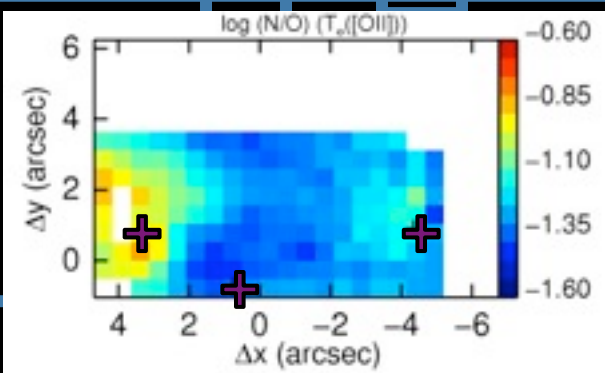
Abundances of heavy elements

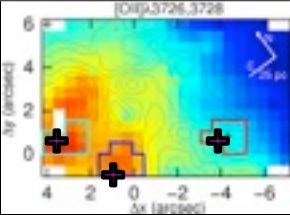


- Oxygen, neon, and argon present homogeneous abundances within 0.1 dex
- Nitrogen abundance has a complex structure with two areas of N-enhancement

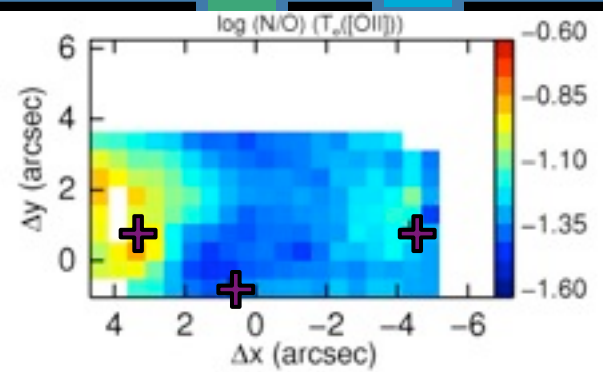


N/O: strong line methods

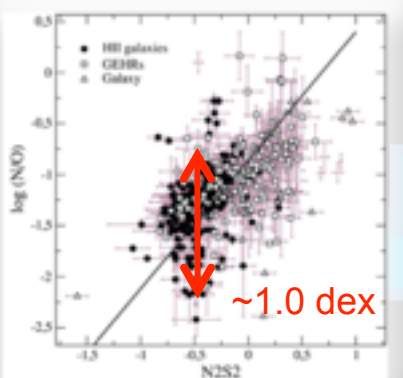
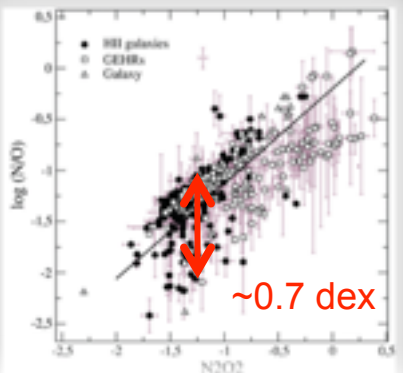
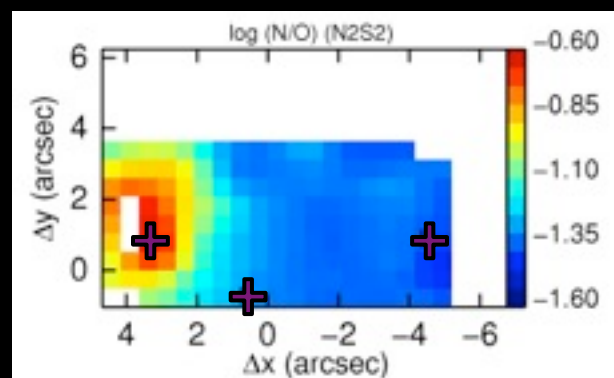
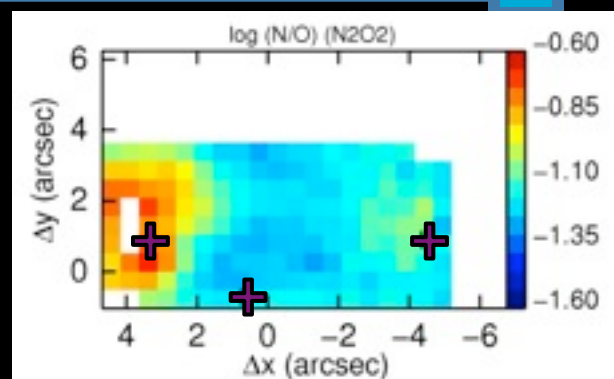
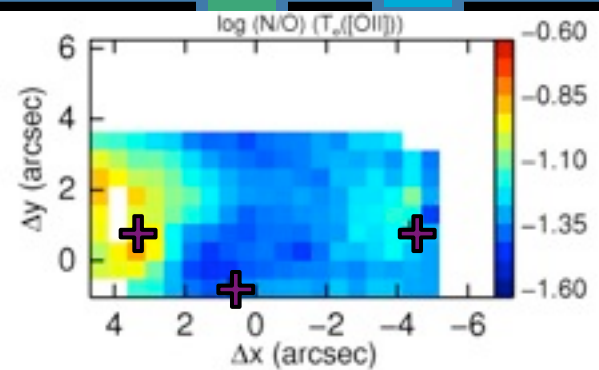
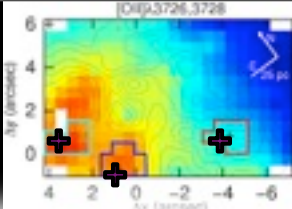




N/O: strong line methods

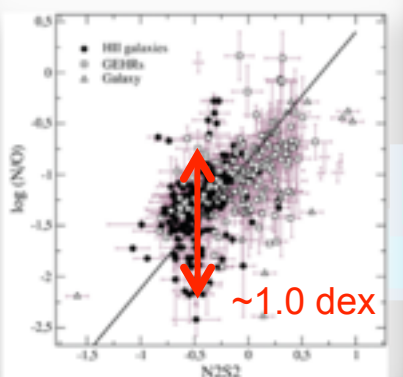
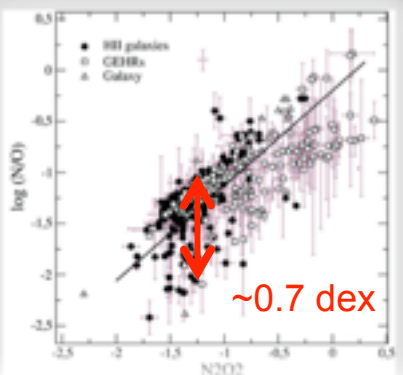
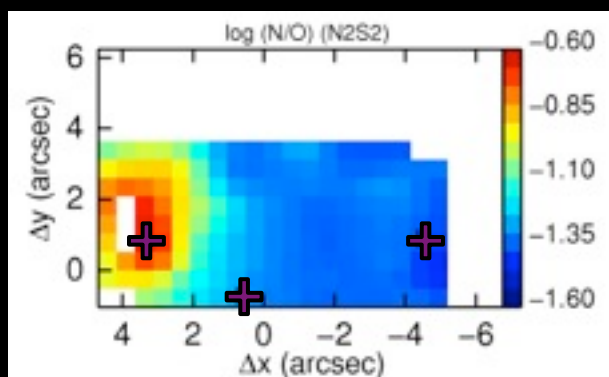
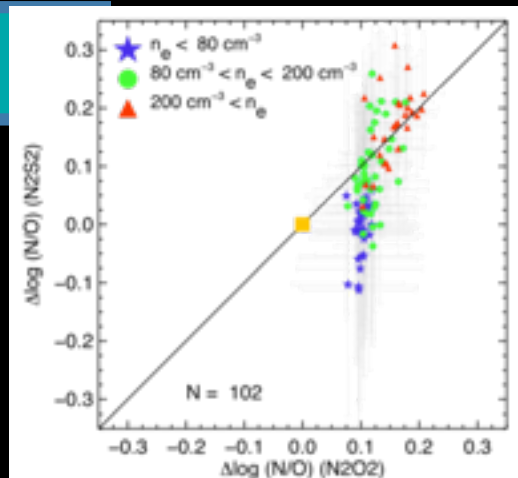
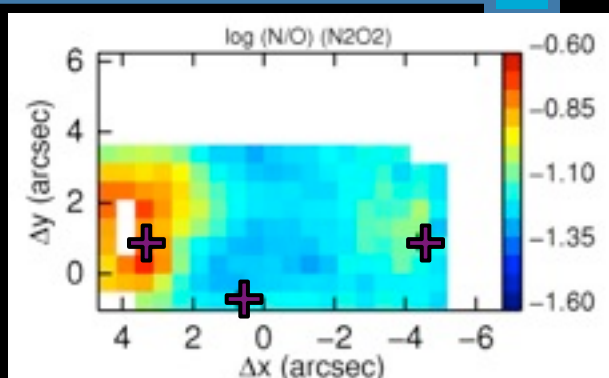
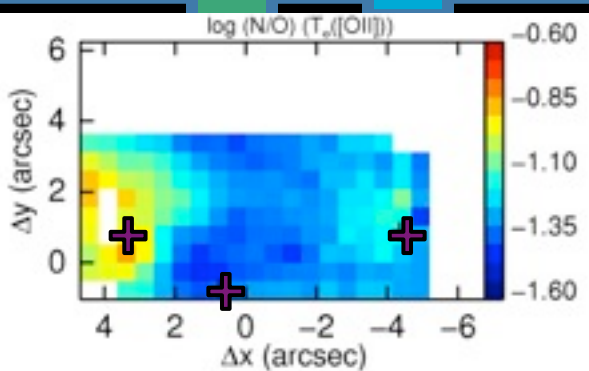
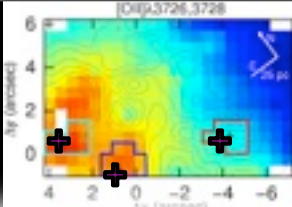


N/O: strong line methods



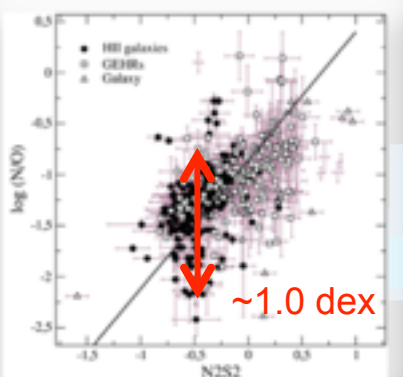
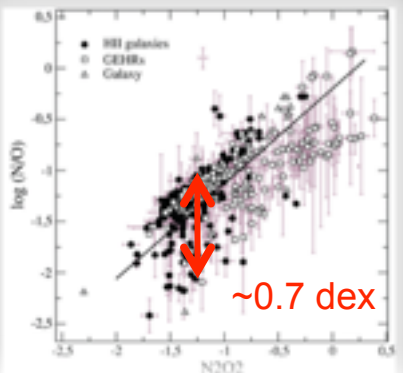
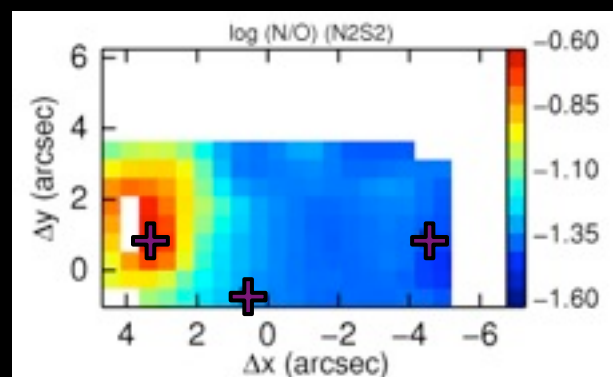
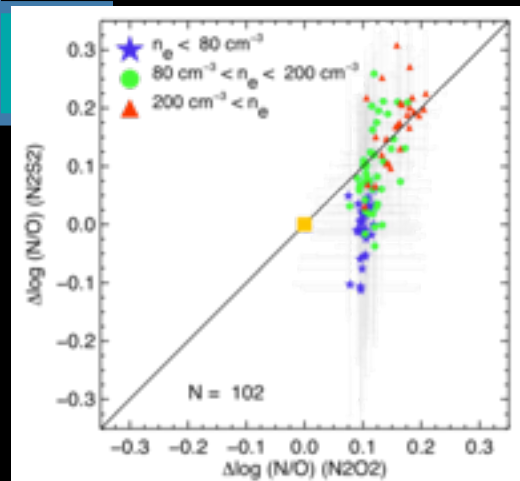
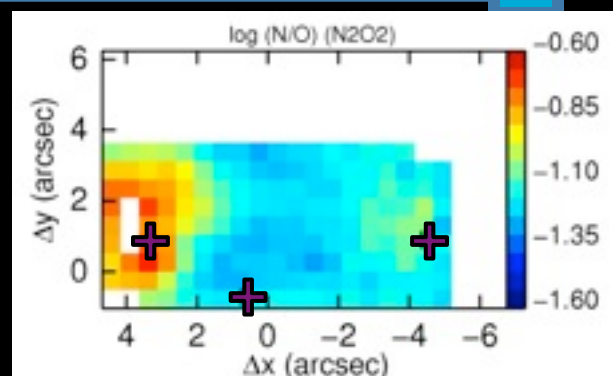
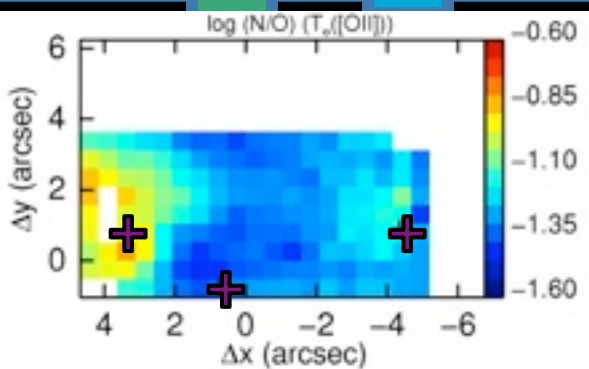
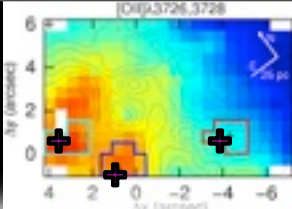
(Pérez-Montero & Contini 2009, MNRAS, 398, 949)

N/O: strong line methods



(Pérez-Montero & Contini 2009, MNRAS, 398, 949)

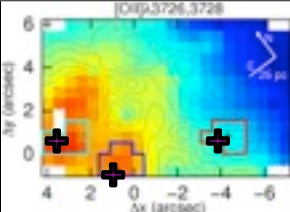
N/O: strong line methods



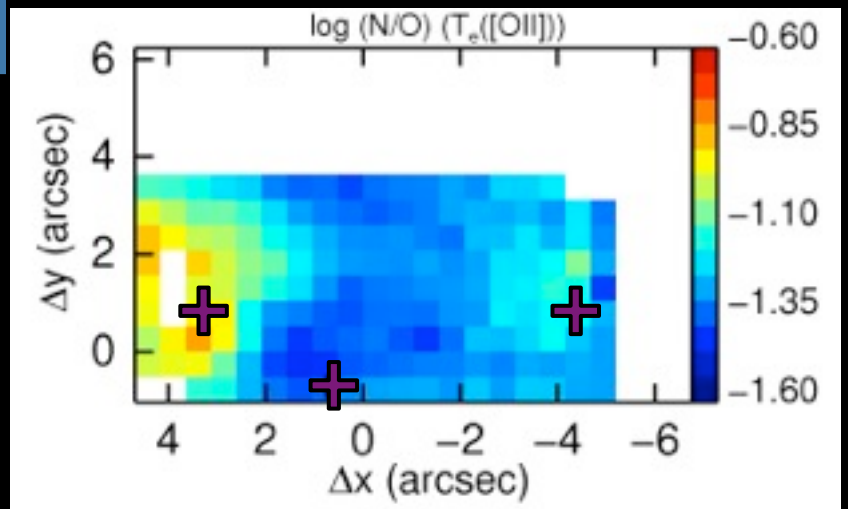
(Pérez-Montero & Contini 2009, MNRAS, 398, 949)

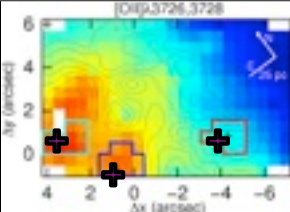
- N2O2 seems more sensitive to small inhomogeneities than N2S2
- N2O2 seems less sensitive to any physical condition than N2S2

Our results support the use of N2O2 over N2S2 to look for N/O inhomogeneities *within* a galaxy

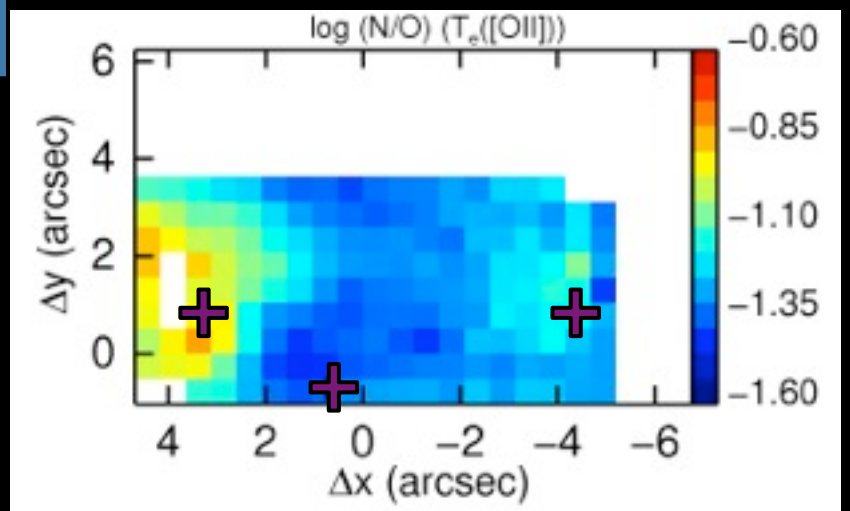


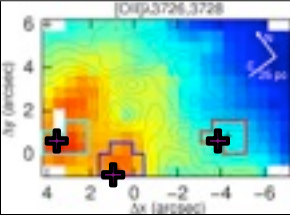
N/O: extra N and WR





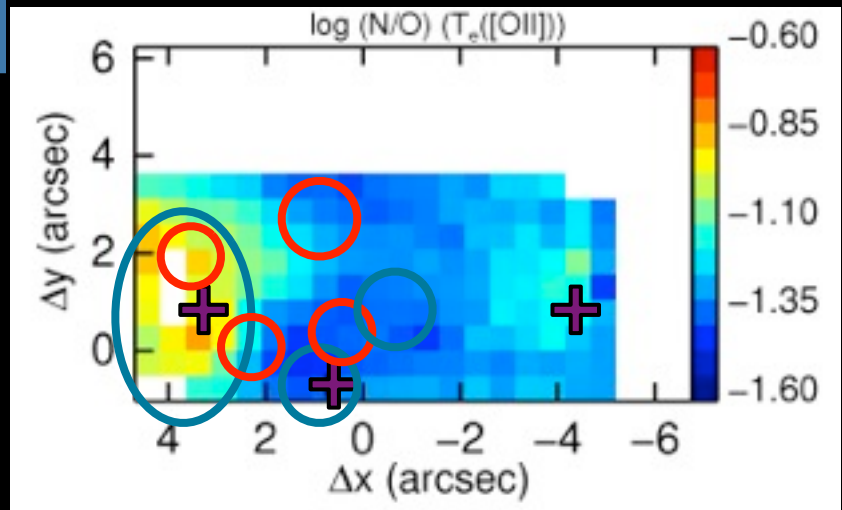
N/O: extra N and WR





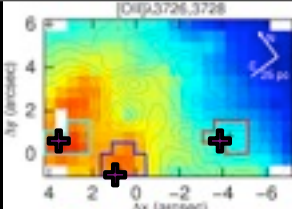
N/O: extra N and WR

WN
WC

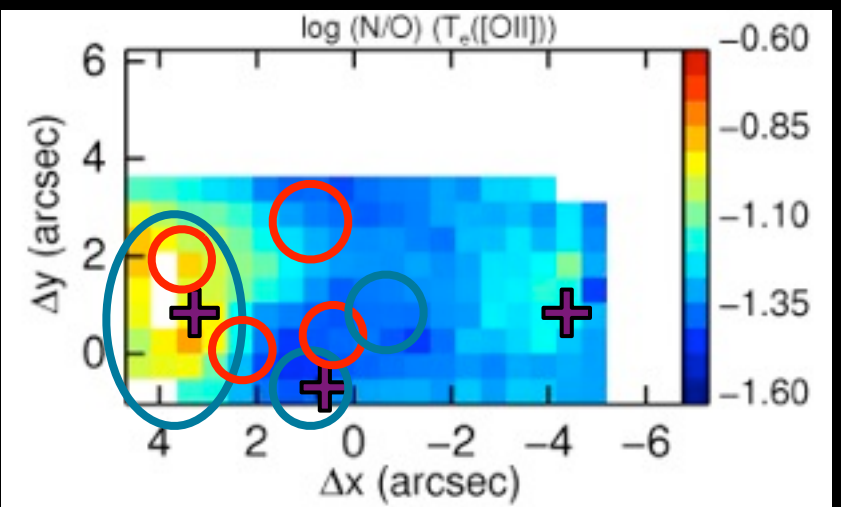


(WN from Montreal-Ibero et al. 2010, A&A, 517, A27
and WC from Westmoquette et al. In prep)

N/O: extra N and WR



WN
WC



(WN from Montreal-Ibero et al. 2010, A&A, 517, A27
and WC from Westmoquette et al. In prep)

- C3: $4.2 \times 10^4 M_{\odot}$; 8 Myr
- C5: $2.1 \times 10^4 M_{\odot}$; 11 Myr
- No WR emission
- With extra-N

- C4: $2.7 \times 10^4 M_{\odot}$; 1 Myr
- C8: $1.3 \times 10^4 M_{\odot}$; 5 Myr
- With WR emission
- No extra-N

(ages and masses from Harris et al.
2004, ApJ, 603, 503, and Alonso-
Herrero et al. 2004, ApJ, 612, 222)

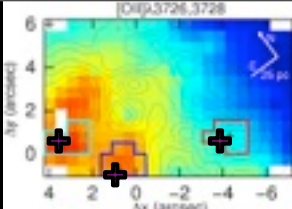
- C1: $5 \times 10^4 M_{\odot}$; 3 Myr
- C2: $\sim 1.0 \times 10^6 M_{\odot}$; 3 Myr
- With WR emission
- With extra-N

#3

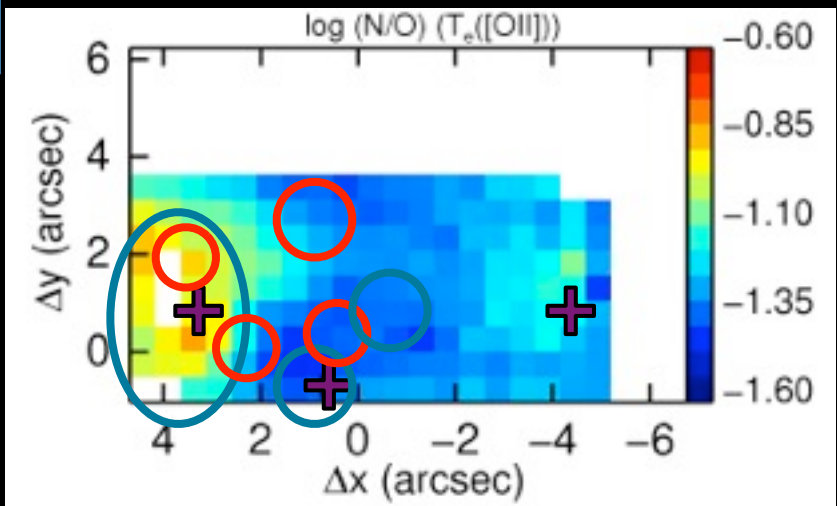
#2

#1

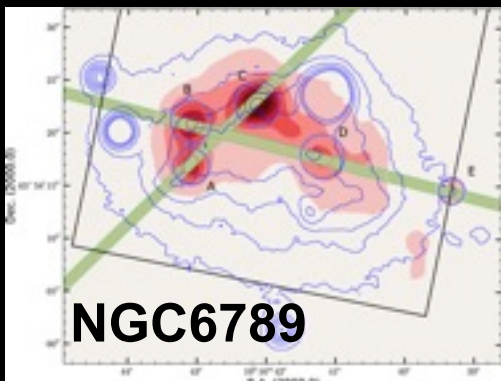
N/O: extra N and WR



WN
WC



(WN from Montreal-Ibero et al. 2010, A&A, 517, A27
and WC from Westmoquette et al. In prep)



- C1: $5 \times 10^3 M_{\odot}$; 3 Myr
- No WR emission
- With extra-N

(García-Benito & Pérez-Montero
2012, MNRAS, 423, 406)

- C3: $4.2 \times 10^4 M_{\odot}$; 8 Myr
- C5: $2.1 \times 10^4 M_{\odot}$; 11 Myr
- No WR emission
- With extra-N

- C4: $2.7 \times 10^4 M_{\odot}$; 1 Myr
- C8: $1.3 \times 10^4 M_{\odot}$; 5 Myr
- With WR emission
- No extra-N

(ages and masses from Harris et al.
2004, ApJ, 603, 503, and Alonso-
Herrero et al. 2004, ApJ, 612, 222)

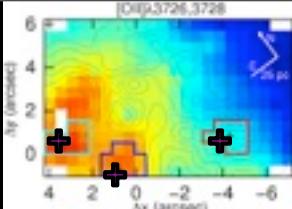
- C1: $5 \times 10^4 M_{\odot}$; 3 Myr
- C2: $\sim 1.0 \times 10^6 M_{\odot}$; 3 Myr
- With WR emission
- With extra-N

#3

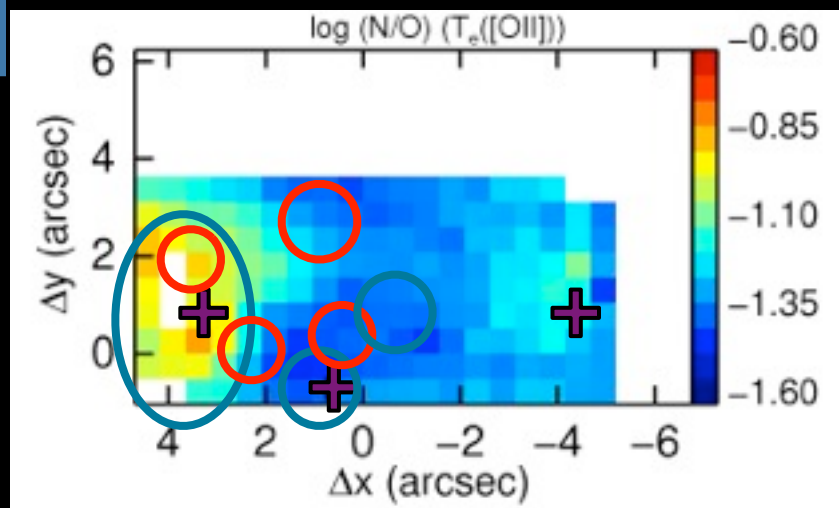
#2

#1

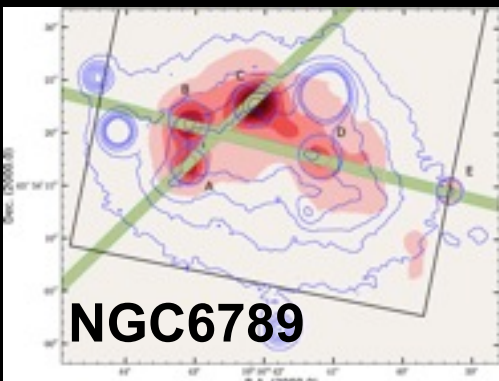
N/O: extra N and WR



WN
WC



(WN from Montreal-Ibero et al. 2010, A&A, 517, A27
and WC from Westmoquette et al. In prep)



NGC6789

- C1: $5 \times 10^3 M_{\odot}$; 3 Myr
- No WR emission
- With extra-N

(García-Benito & Pérez-Montero
2012, MNRAS, 423, 406)

- C3: $4.2 \times 10^4 M_{\odot}$; 8 Myr
- C5: $2.1 \times 10^4 M_{\odot}$; 11 Myr
- No WR emission
- With extra-N

#3

- C4: $2.7 \times 10^4 M_{\odot}$; 1 Myr
- C8: $1.3 \times 10^4 M_{\odot}$; 5 Myr
- With WR emission
- No extra-N

#2

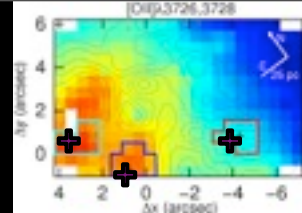
(ages and masses from Harris et al.
2004, ApJ, 603, 503, and Alonso-
Herrero et al. 2004, ApJ, 612, 222)

- C1: $5 \times 10^4 M_{\odot}$; 3 Myr
- C2: $\sim 1.0 \times 10^6 M_{\odot}$; 3 Myr
- With WR emission
- With extra-N

#1

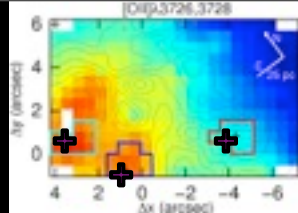
Relationship between WR and N-enhancement is complex

Summary



- Use of 3 n_e tracers allows us to see the 3D structure in n_e . This is “onion-like”. Inner layers denser than outer ones.
- Use of 2 T_e tracers allows us to see the 3D structure in T_e . Higher T_e in the inner layers than in the outer ones.
- Homogeneous abundances for O, Ne, and Ar within $<0.1\text{dex}$
- Two areas of extra N, one of them reported here for the first time.
- N₂O₂ better than N₂S₂ to look for local inhomogeneities.
- Relationship between WR stars and N

Summary



- Use of 3 n_e tracers allows us to see the 3D structure in n_e . This is “onion-like”. Inner layers denser than outer ones.
- Use of 2 T_e tracers allows us to see the 3D structure in T_e . Higher T_e in the inner layers than in the outer ones.
- Homogeneous abundances for O, Ne, and Ar within $<0.1\text{dex}$
- Two areas of extra N, one of them reported here for the first time.
- N₂O₂ better than N₂S₂ to look for local inhomogeneities.
- Relationship between WR stars and N